Redox Biology 11 (2017) 297–311

Contents lists available at ScienceDirect

Redox Biology

journal homepage: www.elsevier.com/locate/redox

The mitochondria-targeted antioxidant MitoQ ameliorated tubular injury mediated by mitophagy in diabetic kidney disease via Nrf2/PINK1

Li Xiao[a,*], Xiaoxuan Xu[a], Fan Zhang[a], Ming Wang[a], Yan Xu[a], Dan Tang[a], Jiahui Wang[a], Yan Qin[a], Yu Liu[a], Chengyuan Tang[a], Liyu He[a], Anna Greka[b], Zhiguang Zhou[c], Fuyou Liu[a], Zheng Dong[a,d], Lin Sun[a]

[a] Department of Nephrology, 2nd Xiangya Hospital, Central South University, Changsha, Hunan, China
[b] Renal Division, Department of Medicine and Glom-NExT Center for Glomerular Kidney Disease and Novel Experimental Therapeutics, Brigham and Women's Hospital, Harvard Medical School, Boston, MA, USA
[c] Department of Endocrinology and Metabolism, 2nd Xiangya Hospital, Central South University, Changsha, Hunan, China
[d] Department of Cellular Biology and Anatomy, Augusta University, Augusta, GA, USA

ARTICLE INFO

Keywords:
Mitoq
Diabetic kidney disease
Mitophagy
Tubular

ABSTRACT

Mitochondria play a crucial role in tubular injury in diabetic kidney disease (DKD). MitoQ is a mitochondria-targeted antioxidant that exerts protective effects in diabetic mice, but the mechanism underlying these effects is not clear. We demonstrated that mitochondrial abnormalities, such as defective mitophagy, mitochondrial reactive oxygen species (ROS) overexpression and mitochondrial fragmentation, occurred in the tubular cells of db/db mice, accompanied by reduced PINK and Parkin expression and increased apoptosis. These changes were partially reversed following an intraperitoneal injection of mitoQ. High glucose (HG) also induces deficient mitophagy, mitochondrial dysfunction and apoptosis in HK-2 cells, changes that were reversed by mitoQ. Moreover, mitoQ restored the expression, activity and translocation of HG-induced NF-E2-related factor 2 (Nrf2) and inhibited the expression of Kelch-like ECH-associated protein (Keap1), as well as the interaction between Nrf2 and Keap1. The reduced PINK and Parkin expression noted in HK-2 cells subjected to HG exposure was partially restored by mitoQ. This effect was abolished by Nrf2 siRNA and augmented by Keap1 siRNA. Transfection with Nrf2 siRNA or PINK siRNA in HK-2 cells exposed to HG conditions partially blocked the effects of mitoQ on mitophagy and tubular damage. These results suggest that mitoQ exerts beneficial effects on tubular injury in DKD via mitophagy and that mitochondrial quality control is mediated by Nrf2/PINK.

1. Introduction

Diabetic kidney disease (DKD) is the leading cause of end-stage renal disease. [1] Tubular injury plays a critical role in DKD progression, which correlates with renal functional deterioration, a primary change associated with the disease. [2] The pathogenesis of DKD is not clear, but mitochondrial abnormalities largely contribute to its development. [3–5].

Mitochondria are dynamic organelles that undergo frequent fission and fusion events modulated by profission proteins (Drp1 and Fis1) and profusion proteins (Mfn1/2 and OPA1), which maintain mitochondrial turnover and cellular network balance. [3] Dysfunctional mitochondria exhibit fragmentation and membrane depolarization, generate massive amounts of reactive oxygen species (ROS) and release apoptogenic proteins (e.g., caspase-3) in response to stressors, such as diabetic nephropathy, which eventually activate the mitochondrial cell death pathway. Renal proximal tubular cells contain an enrichment of mitochondria and rely on oxidative phosphorylation. Therefore, tubules are vulnerable to mitochondrial impairment. [4] Accumulating data indicate that excessive mitochondrial oxidative stress and aberrant dynamics are the primary factors responsible for tubule damage in DKD. [3,6–9] However, the mechanism underlying this process is not fully understood.

Selective macroautophagic (mitophagic) targeting of damaged or dysfunctional mitochondria via PTEN-induced putative kinase 1(PINK)/Parkin-dependent and independent (e.g., BNIP3 and FUNDC1) pathways has been emphasized in recent years. [10,11] These pathways play an essential role in maintaining mitochondrial turnover and quality control. [10,12] Zhan M et al. recently observed decreased tubular cell mitophagy in high-glucose (HG) ambient and

* Corresponding author.
E-mail address: xiaoliznd x@163.com (L. Xiao).

http://dx.doi.org/10.1016/j.redox.2016.12.022
Received 5 November 2016; Received in revised form 9 December 2016; Accepted 19 December 2016
Available online 21 December 2016
2213-2317/

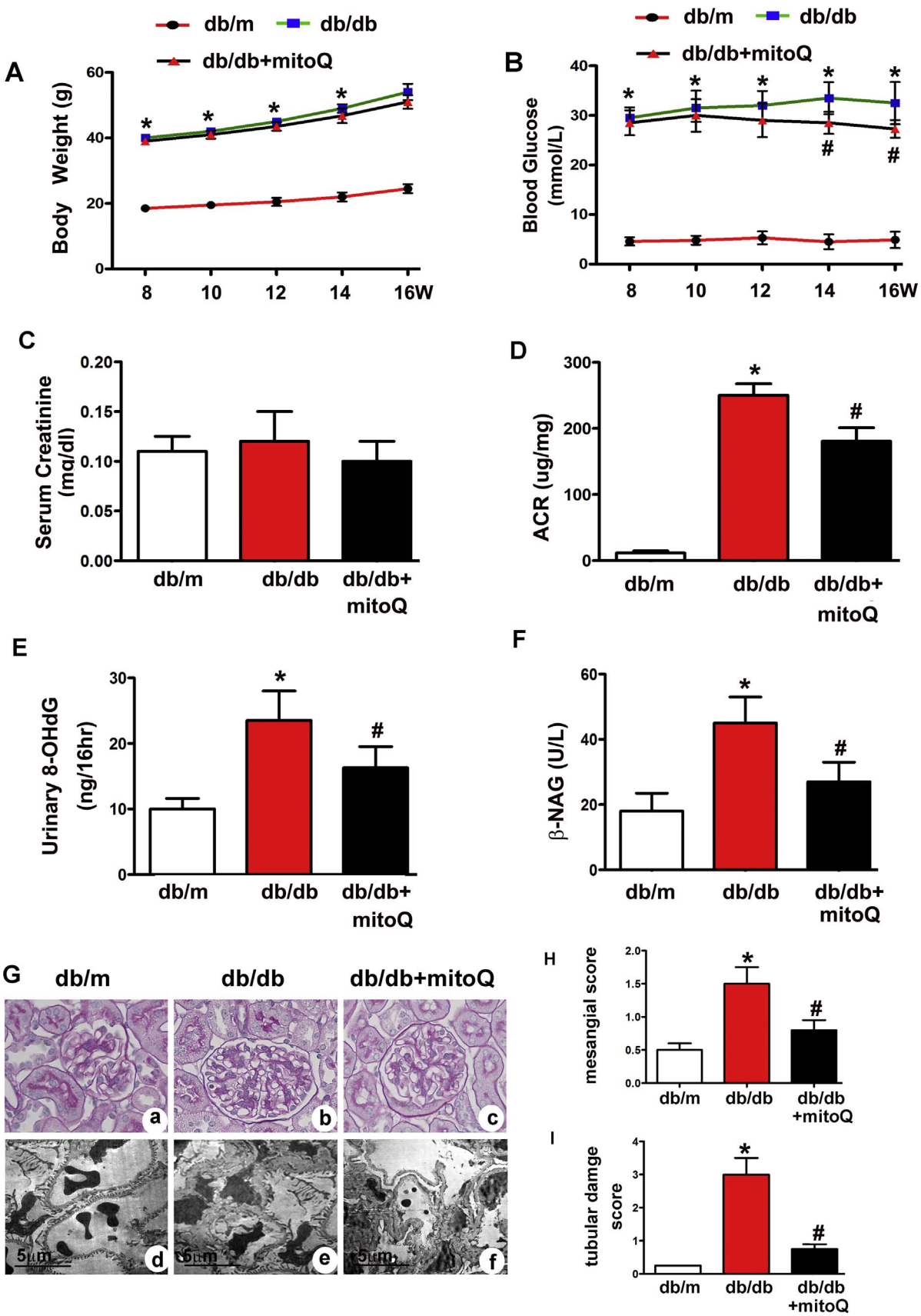

Fig. 1. Effect of mitoQ on renal functional and morphological characteristics in db/db mice. A: Body weight changes in db/m, db/db and db/db mice receiving mitoQ treatment for 8–16 weeks. B: Blood glucose concentrations in each group. C: Serum creatinine levels. D: Urinary ACRs. E and F: Urinary excretion of 8-OHdG and urine β-NAG levels. G: PAS staining (top panels) and EM (bottom panels) showing notable deformations in the tubules and glomeruli of db/db mice compared to those of db/m mice (Gb vs. Ga and Ge vs. Gd). These changes were dramatically ameliorated by mitoQ administration (Gc vs. Gb and Gf vs. Ge). H and I: Quantitative analysis of mesangial scores and tubular damage in each group. Values are the mean ± SE, *P < 0.05 vs. db/m; #P < 0.05 vs. db/db mice. n=6.

the kidneys of STZ-induced diabetic mice, a process that was mediated by myo-inositol oxygenase (MIOX) via PINK/Parkin and was negatively correlated with ROS overproduction, mitochondrial fragmentation and apoptosis. [3] Huang CH et al. demonstrated that mitophagy inhibition was associated with tubular damage via the thioredoxin interacting protein (TXNIP)/mTOR/BNIP3 signaling pathway in dia-

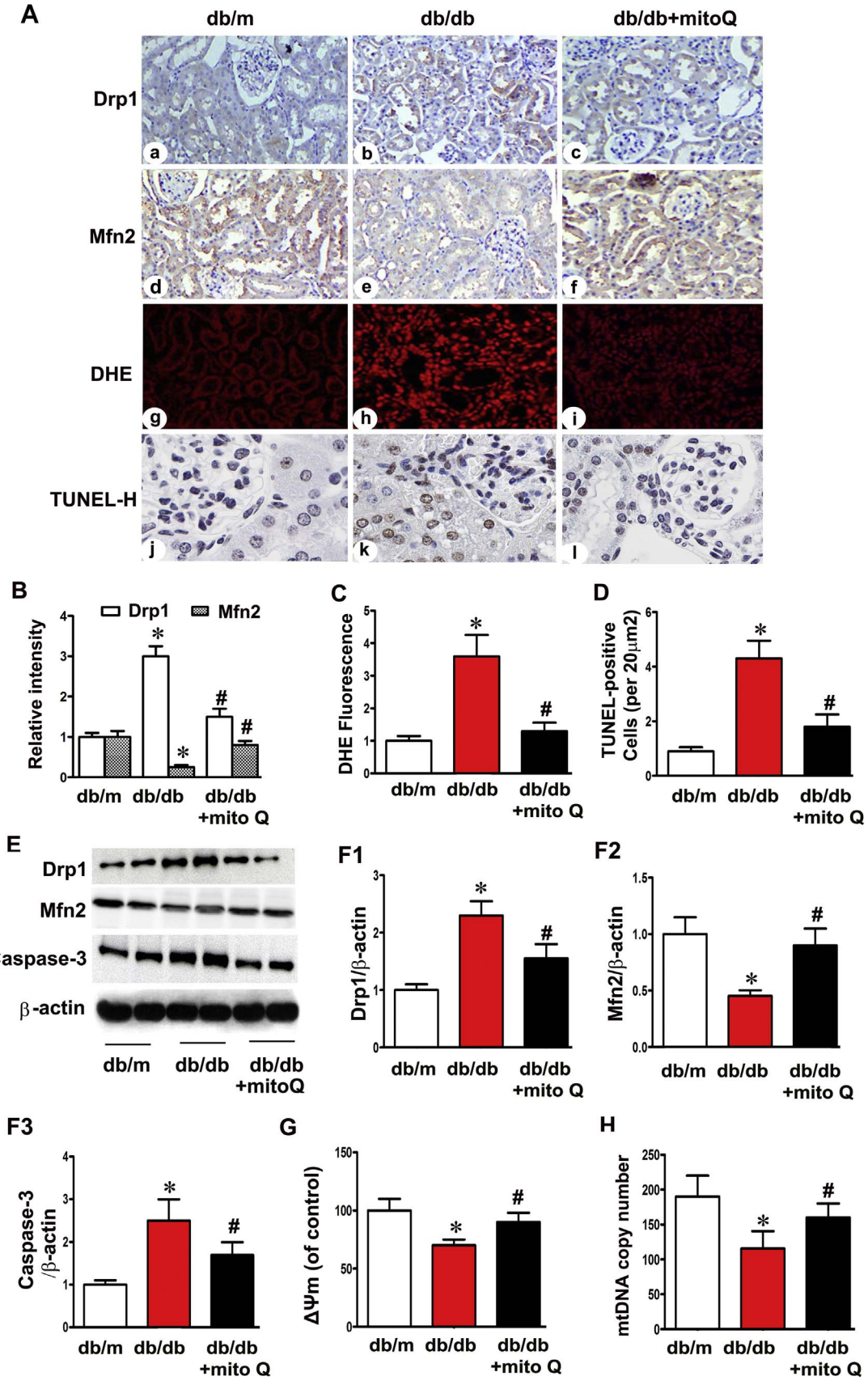

Fig. 2. Restoration of mitochondrial dynamic-related protein expression, oxidative stress, mitochondrial membrane potential and apoptosis in the tubules of db/db mice after mitoQ administration. A: Profission protein Drp1 (a–c) and profusion protein Mfn2 (*d*-f) expression levels were assessed using IHC in db/m, db/db and db/db mice treated with mitoQ (magnification ×400). Oxidative stress and apoptosis in kidney tubular cells were assessed using DHE (*g*-i) and TUNEL-H staining (j-l). B: Semiquantification of IHC staining of Drp1 and Mfn2. C and D: Quantification of tissues stained with DHE and TUNEL-H. E: Western blotting assay showing that Drp1 (top panels) and cleaved caspase-3 (bottom panels) expression levels increased in the kidneys of db/db mice compared to those of db/m mice. These effects were reversed by mitoQ treatment. MitoQ also restored Mfn2 expression (middle panels) in db/db mice. F1-F3: Quantification of the average band densities calculated from different Western blots. G and H: Bar graphs depicting mitochondrial voltage potential (△Ψm) and mitochondrial DNA (mtDNA) copy numbers in the tubular cells of the kidneys in the three groups. Values are the mean ± SE. *P < 0.05 vs. db/m; #P < 0.05 vs. db/db mice. n=6.

betic mice. [13] Therefore, the present study examined the maintenance of mitochondrial quality control via mitophagy using a pharmacological method to decrease mitochondrial oxidative damage and protect against tubular damage in a hyperglycemic state.

The mitochondria-targeted antioxidant mitoQ comprises coenzyme Q10 and TPP cations, which makes it several hundred-fold more potent than an untargeted antioxidant with respect to the prevention of mitochondrial oxidative damage. [14] MitoQ plays a protective role in various diseases, such as neurodegenerative disease, cardiac hypertrophy, and liver fibrosis. [15–18] MitoQ effectively prevented inflammatory damage in hepatitis virus patients in a phase 2 clinical trial. [19] Emerging data indicate that mitoQ may exert beneficial effects on tubular injury under various conditions. [20–22] MitoQ prevents tubular damage from cold storage [20] and ischemia–reperfusion in animal models [21] and improves tubular dysfunction in type I diabetic mice. [22].

Notably, a recent study demonstrated that MDA-MB-231 breast cells underwent autophagy following treatment with mitoQ, a process that was modulated by the crucial oxidative stress regulator NF-E2-related factor 2 (Nrf2)/Kelch-like ECH-associated protein (Keap1). [23] However, the precise mechanism(s) by which mitoQ prevents tubular damage under hyperglycemic conditions is not clear.

This communication describes the effects of mitoQ on appropriated tubular injury in the kidneys of db/db mice and verifies the mechanisms underlying the regulation of mitophagy and mitochondrial oxidative stress and dynamics by mitoQ in HK-2 cells exposed to HG conditions.

2. Research design and methods

2.1. Animal experimental design

Twelve-week-old male C57BL/6 J db/db and C57BL/6 J db/m mice were used for the animal experiments. These mice were purchased from the Aier Matt Experimental Animal Company (Suzhou, China). They were organized into the following three groups for the animal experiments: a db/m group (control, n=12), a db/db group (n=12) and a db/db group receiving an intraperitoneal injection (i.p.) of mitoQ (Focus Biomolecules, USA, 5 mg/kg, twice weekly for 12 weeks, n=12). The mice were euthanized at 24 weeks of age. The Animal Care and Use Committee of Second Xiangya Hospital of Central South University approved all animal procedures.

2.2. Assessment of physiological features and renal function

Body weights were measured, and blood, serum, and urine sample collection was performed every two weeks. Blood glucose levels were detected using a blood glucose monitor (Boehringer Mannheim, Mannheim, Germany). Urine albumin concentrations were measured using a mouse urine albumin ELISA kit (Bethyl Laboratories, USA), and serum creatinine levels were tested using a QuantiChrom Creatinine Assay Kit (BioAssay Systems, USA), according to the manufacturer's protocol. Urinary ACR was calculated as the urine albumin/creatinine ratio. Urine β-NAG was measured using an automated colorimetric method (Pacific Biomarkers, Inc, USA), and urine 8-hydroxy-2-deoxyguanosine (8-OHdG) levels were measured using an 8-OHdG ELISA kit (JaICA, Japan).

2.3. Morphological analysis of kidney tissue and immunohistochemistry (IHC)

Morphological changes in the kidney sections were assessed using periodic acid Schiff (PAS) staining and transmission electron microscopy (TEM). Mesangial expansion scores and tubular damage were analyzed using a semiquantitative scoring system, as previously described. [24,25] Paraffin-embedded kidney sections used for IHC studies were dewaxed, rehydrated, and incubated with primary antibodies overnight at 4 °C. The sections were subsequently incubated with secondary antibodies, treated with diaminobenzidine, counterstained with hematoxylin and examined as previously reported. [3].

2.4. Cell culture studies

The human proximal tubular cell line HK-2 (ATCC, Rockville, USA) was used for our *in vitro* studies. Dose- and time-dependent experiments were performed using 5–45 mM D-glucose for 48 h or 30 mM glucose for 0–48 h. The HK-2 cells were pretreated with mitoQ for 2 h before exposure to 5 mM glucose (LG) or 30 mM glucose (HG) to observe the effects of mitoQ on mitophagy, mitochondrial function and apoptosis. Nrf2 or PINK siRNA and/or Keap1 siRNA were pretransfected into the HK-2 cells using Lipofectamine 2000 reagent (Life Technologies, USA) and were used for our *in vitro* studies.

2.5. Examination of mitophagy and mitochondrial fragmentation using electron microscopy and immunofluorescence assay

Mitochondrial morphology and kidney tubule mitophagy were observed as previously described. [3,26] Briefly, we fixed dissected renal cortices with 2.5% glutaraldehyde. We observed toluidine blue-stained EPON-embedded sections using a TEM (ZEISS 906, Germany) to evaluate mitophagy and the extent of mitochondrial fragmentation. [3,9] We also performed immunofluorescence co-staining using LC3 and VDAC antibodies to delineate the mitophagy in the kidney tubule.

HK-2 cells were stained using Mitotracker and incubated with LC3 (1:100), P62 (1:100) and PINK (1:100) antibodies and secondary antibodies conjugated with Alexa Fluor to monitor mitophagy *in vitro*. These cells were counterstained with 4′,6-diamidino-2 phenylindole (DAPI) (Invitrogen, USA), and their fluorescent signals were visualized using confocal microscopy. The colocalization intensity of LC3, p62 or PINK, as demonstrated by MitoTracker Deep Red, was analyzed using Leica Image analysis software (Leica Microsystems, Germany).

2.6. Measurement of superoxide generation and apoptosis

Superoxide production and apoptosis were detected as described previously. [3,9] Briefly, mitochondrial superoxide generation was detected using MitoSOX Red (Invitrogen, USA). [9] Dihydroethidium (DHE, Invitrogen) and 2′,7′-dichlorodihydrofluorescein diacetate (H2-*DCFDA,* Invitrogen) were used to assess intracellular ROS production in the kidney tubules and HK-2 cells, respectively. [3,9] TUNEL was used to measure apoptosis, according to the manufacturer's instructions. [3,7].

2.7. Assessment of mitochondrial transmembrane potential (△Ψm), mtDNA copy numbers and ATP activity

Mitochondrial transmembrane potential (△Ψm) in HK-2 cells and

kidney tubules was assessed as described previously. [9] Briefly, 10 nmol/L TMRE dye (Molecular Probes) was added to HK-2 cell medium for 10 min and assessed via fluorescence-activated cell sorter (FACS) analysis and confocal microscopy at a wavelength of 582 nm. The △Ψm in mitochondria isolated from renal tissue samples was measured using a load of rhodamine 123 (Sigma-Aldrich, USA) and was

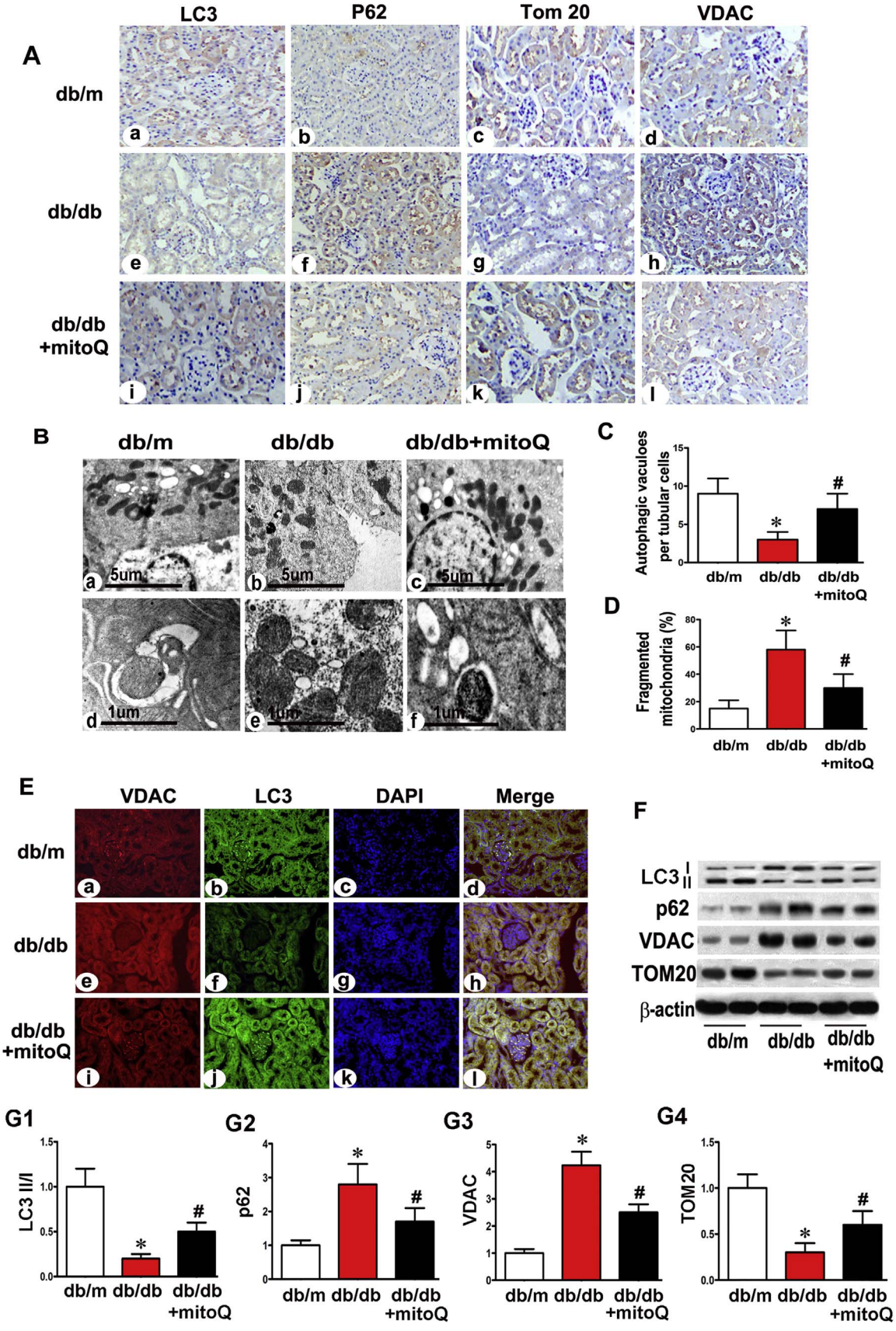

Fig. 3. Restoration of abnormal mitophagy in the proximal tubules in db/db mice treated with mitoQ. A: Kidney sections from db/m mice, db/db mice and db/db mice subjected to mitoQ treatment were stained with LC3 (column 1), p62 (column 2), TOM20 (column 3) and VDAC (column 4) antibodies for IHC analysis (magnification ×400). B: Using a TEM, we observed autophagic vacuoles observed in db/m mice. We observed less vacuoles in the tubular cells of db/db mice than in those of other mice (top panels, Bb vs. Ba). These vacuoles were restored in mice treated with mitoQ (Bc vs. Bb). Higher magnification TEM revealed mitophagy, which was visualized as autophagosome-containing mitochondria in db/m mice and db/db mice administered mitoQ (bottom panels). C and D: The bar graph represents quantification of the numbers of autophagic vacuoles in each tubular cell and fragmented mitochondria. E: Immunofluorescence demonstrating LC3 and VDAC colocalization in the kidney tubules of db/m mice stained with LC3 (green) and VDAC (red) antibodies (top panels). LC3 intensity decreased in the tubular cells of kidneys in db/db mice compared to those in db/m mice (Ef vs. Eb). This intensity was restored by mitoQ administration (Ej vs. Ef). Contrasting intensity changes were observed with respect to VDAC expression (column 1). F: Western blot analysis of LC3, p62, TOM20 and VDAC expression. G1-G4: Quantification of average Western blot band intensities. Values are the mean ± SE. *P < 0.01 vs. db/m; #P < 0.01 vs. db/db. n=6.

calculated as discussed previously. [9,27].

MtDNA was extracted and measured as previously described. [28] Briefly, mtDNA was extracted from mouse tubular cells using a commercial kit (Qiagen, USA) and measured using real-time PCR with an SYBR Green Kit (Pierce, USA). Mitochondrial ATP activity was assayed using a ATP bioluminescence assay kit (Roche Diagnostics, Switzerland), according to the manufacturer's instructions. [13].

2.8. Nrf2 nuclear translocalization and activity assay

HK-2 cells were plated on coverslips, exposed to HG with or without mitoQ treatment, and stained with anti-Nrf2 and secondary antibodies. Cell nuclei were stained with DAPI, and Nrf2 translocation was observed using confocal microscopy. [27] Nrf2-antioxidant response element (ARE) binding was measured using a TransAM Nrf2 Kit (active motif), as previously described. [29] Briefly, 10 μg of nuclear protein was incubated in a 96-well plate and coated with oligonucleotides containing a consensus binding site for Nrf2. The plate was incubated with an anti-Nrf2 antibody and HRP-conjugated secondary antibody. The absorbance was measured at 450 nm and reflected Nrf2 activity. [29].

2.9. PINK1 mRNA expression, as assessed using real-time PCR

HK-2 cells were pre-transfected with Keap1 siRNA and/or Nrf2 siRNA (QIAGEN) for 30 min using Lipofectamine, subjected to HG exposure, and treated with or without mitoQ for 24 h. A control siRNA (QIAGEN) was used as a negative control. PINK1 mRNA expression levels were determined using real-time PCR, as previously reported. [30] The PINK mRNA assay ID was obtained from Applied Biosystems (Hs00260868_m1). The probe was targeted to position 483 of the mRNA sequence (GenBank accession number NM_032409) and normalized to GAPDH. Expression was calculated using the $2^{-\Delta\Delta Ct}$ method.

2.10. Western blotting and coimmunoprecipitation (IP) studies

Total cell lysates and cytoplasmic and nuclear extracts were isolated from the cells for Western blot assays, as described previously. [3] Proteins were separated using 10% SDS-PAGE and transferred to PVDF membranes, which were probed with primary antibodies against Drp1, Mfn2, Pink1, Nrf2, Parkin, TOM20 and VDAC (Santa Cruz Biotechnology, USA), LC3I/II, cleaved caspase-3 (Cell Signaling Technology, USA), p62 (Abcam, USA) and Keap1 (Proteintech, USA) and developed using an ECL system (Amersham Biosciences, USA). β-Actin (Santa Cruz) and histone 3 (Novus Biologicals, USA) were used as internal controls.

Each sample was adjusted to 1 mg/ml and divided into two equal aliquots containing 100 μg of protein to observe the interaction between Keap1 and Nrf2 via IP, as described previously. [7] The samples were incubated with an anti-Nrf2 or anti-Keap1 antibody in an IP buffer for 12 h at 4 °C. Protein A-sepharose beads (50 μl) were added to the samples, which were incubated for another 12 h. The samples were then washed and resuspended, and Western blotting was performed as described previously. [7].

3. Results

3.1. Effects of MitoQ on renal function and morphological changes in db/db mouse kidneys

Db/db mice exhibited higher body weights, increased urinary ACRs and increased blood glucose and serum creatinine, 8-OHdG and β-NAG levels compared to db/m mice (Fig. 1**A–F**). Notable decreases in the urinary ACR and in 8-OHdG and β-NAG levels (Fig. 1**D–F**) were observed in db/db mice after mitoQ treatment. A slight reduction in blood glucose levels was observed in db/db mice treated with mitoQ (Fig. 1**B**), but no significant changes in serum creatinine levels were observed in the different groups. PAS staining showed notable morphological changes in the kidneys of db/db mice, including glomerular hypertrophy, increases in mesangial matrix and tubular epithelial disruption (Fig. 1**G a and b**). Furthermore, TEM revealed basement membrane thickening accompanied by extensive foot process fusion (Fig. 1**G d, e**). However, mitoQ treatment dramatically ameliorated these changes (Fig. 1**G c and f**). Quantitative analysis of mesangial scores and tubular damage scores confirmed the alterations in mesangial expansion and tubular damage (Fig. 1**H and I**).

3.2. MitoQ restored the alterations in Drp1 and Mfn2 expression and ameliorated ROS Generation and proximal tubular cell apoptosis in the kidneys of Db/db mice

Drp1 expression intensity was evaluated using IHC, and Drp1 expression was found to be up-regulated in the tubules of db/db mice compared to those of controls, and Mfn2 expression was down-regulated in these mice compared to controls. MitoQ administration significantly inhibited Drp1 expression and restored Mfn2 expression in db/db mice (Fig. 2**A**). Similar results were demonstrated using Western blot assays (Fig. 2**E, F1 and F2**). DHE and TUNEL assays demonstrated concomitant increases in oxidative stress and apoptosis in the tubular cells of the kidneys of db/db mice, and mitoQ significantly reduced these effects (Fig. 2**A, C and D**). Cleaved caspase-3 expression was significantly increased in the tubules of db/db mice, and mitoQ partially inhibited this increase (Fig. 2**E and F3**). Decreased $\triangle\Psi m$ and mtDNA copy numbers were also observed in the kidneys of db/db mice, and mitoQ treatment reversed these changes (Fig. 2**G and H**). These results suggest that mitoQ may play a role in mitochondrial quality control and that this role may underlie the amelioration of tubular oxidative stress and apoptosis in diabetic mice.

3.3. Effect of MitoQ on mitophagy in the proximal tubular cells of Db/db mice

IHC staining of LC3 revealed a significant reduction in its expression in the renal tubules of db/db mice, and mitoQ significantly reversed this change (Fig. 3**A a, e, i**). Conversely, p62 expression was up-regulated in the renal tubules of db/db mice, and mitoQ treatment reversed this change (Fig. 3**A b, f, j**). TOM20 and VDAC are mitochondrial member proteins. TOM20 quantification is widely performed to monitor mitochondrial mass during mitophagy, [31] and VDAC1 degradation by ubiquitination is associated with mitophagy. [32] IHC revealed notably decreased TOM20 expression in the tubules of db/db mice compared to those of controls, and mitoQ treatment

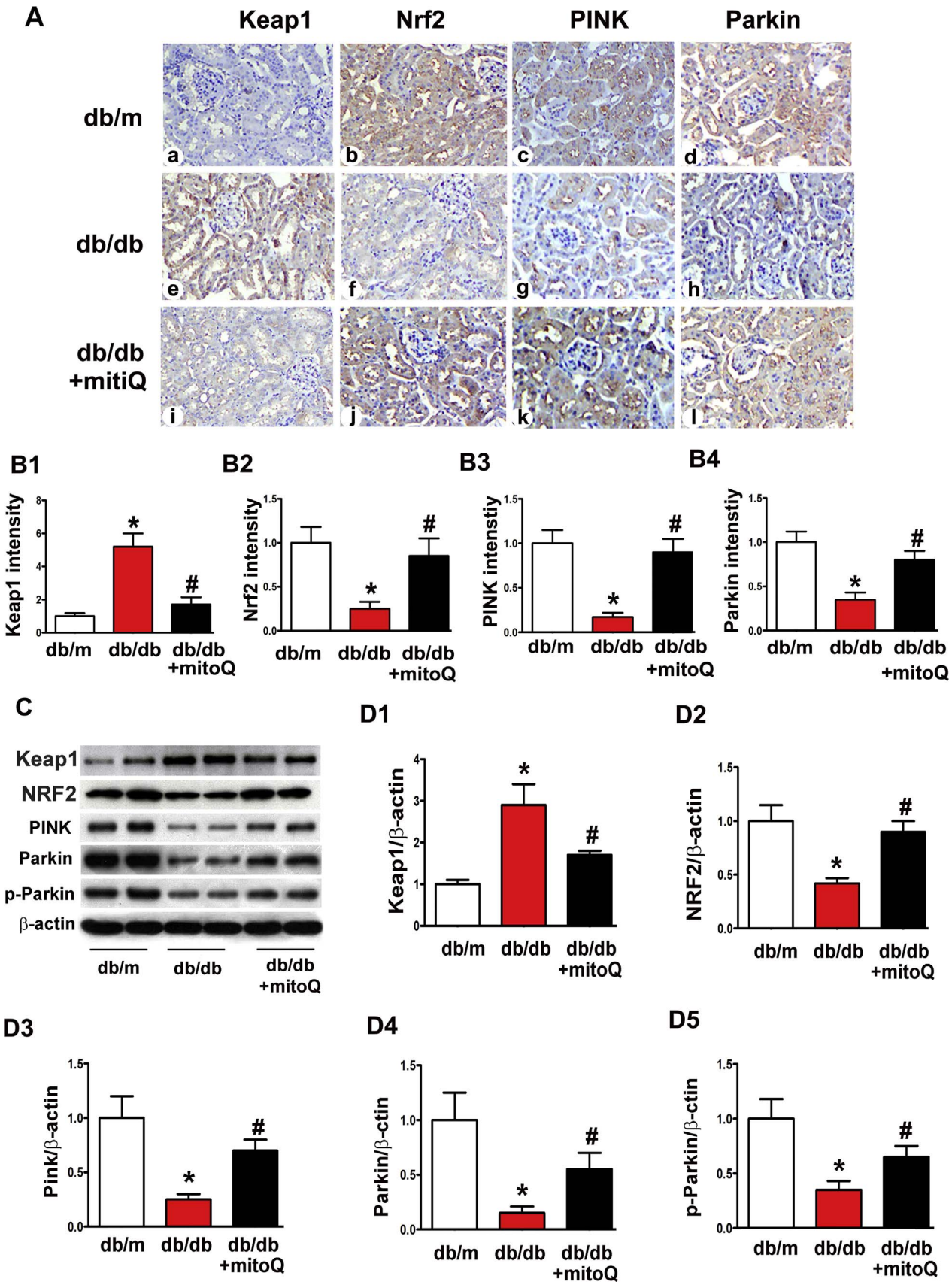

Fig. 4. The effect of mitoQ on the expression of the mitophagy-associated proteins PINK and Parkin and the oxidative stress adaptors Keap1 and Nrf2 in db/db mice. A: IHC, kidney sections in db/m mice, db/db mice and db/db mice treated with mitoQ were stained with Keap1 (column 1), Nrf2 (column2), PINK (column3) and Parkin (column4) antibodies. PINK, Parkin, and Nrf2 intensity decreased in the tubules in the kidneys of db/db mice compared to those of control mice (middle panels vs. top panels). These intensities were restored by mitoQ treatment (bottom panels vs. middle panels). Conversely, Keap1 intensity was increased in db/db mice, but this increase was partially inhibited after mitoQ treatment. B1-B4: Semiquantification of IHC staining of Keap1, Nrf2, PINK and Parkin in kidney tissues. C: Western blot analysis of Keap1, Nrf2, PINK, Parkin and phosphorylated-Parkin (*p*-Parkin) expression. D1-D5: Quantification of average Western blot band intensity. Values are the mean ± SE. *P < 0.01 vs. db/m; #P < 0.01 vs. db/db. n=6.

reversed this change (Fig. 3**A c, g, k**). A contrasting result was observed with respect to VDAC expression (Fig. 3**A d, h, l)**. TEM revealed reduced numbers of autophagic vacuoles in the tubular cells of db/db mice, an effect that was partially reversed by mitoQ treatment. High-magnification electron micrographs revealed that most of the tubular cells in db/m mice exhibited elongated cylindrical-shaped

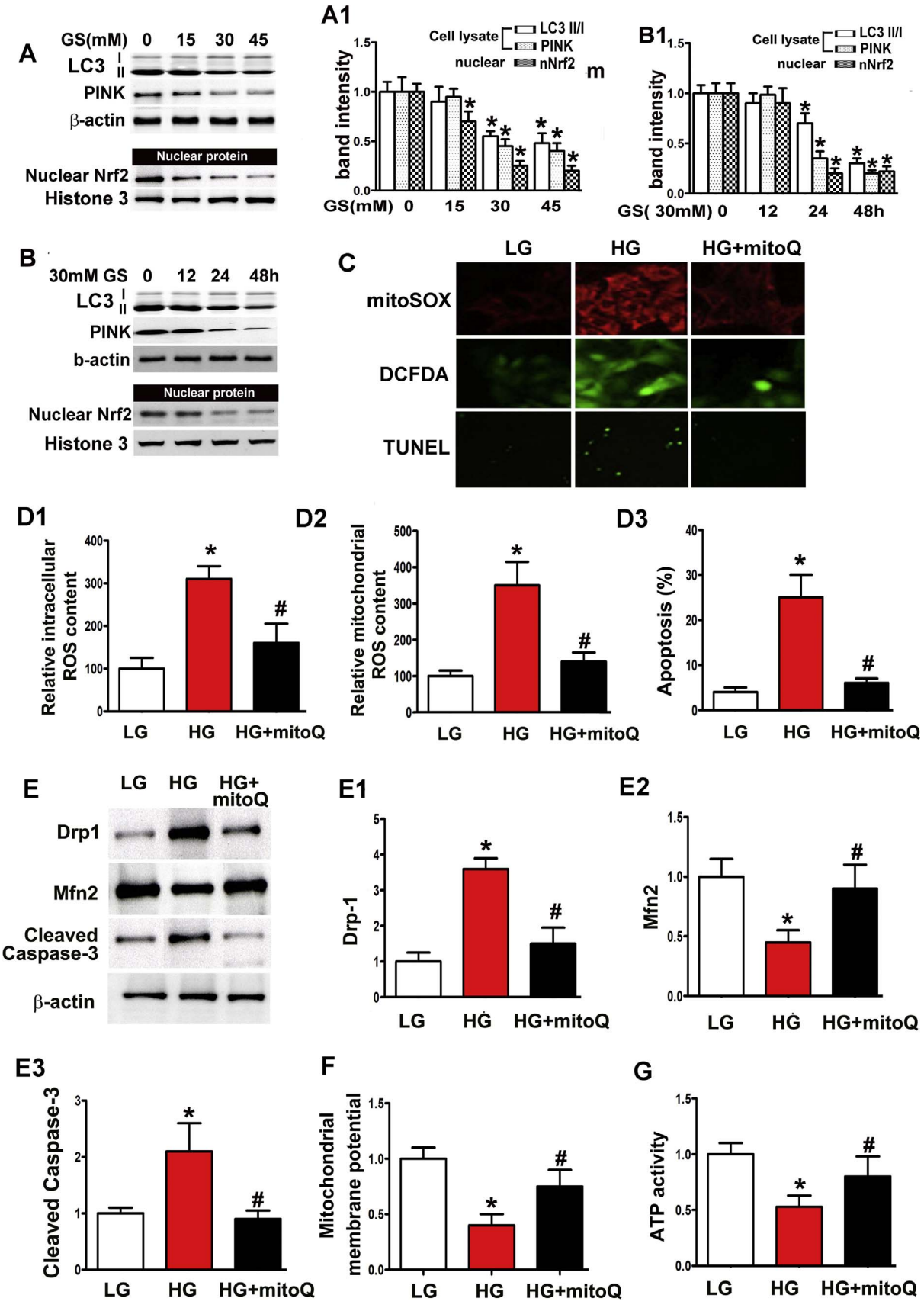

Fig. 5. Protective effects of mitoQ on mitochondrial damage in HK-2 cells subjected to HG exposure. A: Immunoblot assay for LC3II, PINK and nuclear Nrf2 expression in HK2 cells subjected to various concentrations of HG (0–45 mM) for 48 h. Dose dependent decreases in the expression of these proteins were observed in HK-2 cells treated with HG. B: LC3II, PINK and nuclear Nrf2 expression, as determined by Western blotting, in HK2 cells subjected to 30 mM HG exposure for different times (0–48 h), which induced a time-dependent decrease in protein expression. A1 and B1: Quantification of average band intensities using Western blotting. C: Confocal microscopic images revealing the levels of mitochondrial ROS (top panels), intracellular ROS (middle panels) and apoptosis (bottom panels) in HK-2 cells under low glucose (5 mM, LG) and HG exposure (30 mM) with or without mitoQ. D1-D3: Quantification of intracellular ROS, mitochondrial ROS and apoptotic cells, which was performed using H2-DCFDC, MitoSOX and TUNEL-F assays. E: Immunoblot assays of Drp1 (top panels), Mfn2 (middle panels) and cleaved caspase-3 (bottom panels) expression in HK-2 cells subjected to HG exposure. E1-E3: Quantification of average Western blot band intensities. F and G: Bar graphs revealing the mitochondrial membrane potential and ATP activity of HK-2 cells incubated under HG conditions. Values are the mean ± SE. *P < 0.01 vs. LG; #P < 0.01 vs. HG. n=3.

mitochondria. However, approximately 60% of the tubular cells in db/db mice exhibited fragmented mitochondria, a change that was partially reversed by mitoQ treatment (Fig. 3**B a-c, 3D**). Autophagosome-engulfing mitochondria are an indicator of mitophagy, and these structures were observed in the tubular cells of db/m mice and db/db mice treated with mitoQ supplementation but were not observed in db/db mice without treatment (Fig. 3**B d-f**). The numbers of autophagic vacuoles were reduced in the tubular cells of db/db mice compared to those of db/m mice. These effects were partially reversed in the tubules of mice treated with mitoQ (Fig. 3**C**).

Confocal microscopic images revealed LC3 and VDAC colonization in the tubules of db/m mice. Decreased LC3 (green) intensity and increased VDAC (red) intensity were observed in db/db mice compared to db/m mice. These effects were reversed by mitoQ (Fig. 3**E**). It has been suggested that the conversion of LC3I to LC3II may represent autophagosome formation, and the LCII/LC3I ratio has been used to monitor autophagy levels via immunoblotting. [33,34] As expected, results similar to those described above were observed using Western blot assays to evaluate the LCII/LC31 ratio and TOM20 expression. MitoQ reversed the decreases in the LC3II/LC3I ratio and TOM20 expression that were noted in db/db mice, as shown via immunoblotting. Moreover, mitoQ inhibited the increases in p62 and VDAC expression (Fig. 3**F and G1-G4**).

3.4. Effect of MitoQ on the expression of mitophagy-associated proteins, Keap1 and Nrf2

The mitophagy-associated proteins PINK and Parkin were investigated using IHC to examine the mechanisms underlying the effects of mitoQ on tubular cell mitophagy in db/db mice. Decreased PINK and Parkin protein expression levels were observed in the tubules of db/db mice. These changes were reversed by mitoQ treatment (Fig. 4**A, B3 and B4**). Similar results were observed with respect to PINK, Parkin and phosphorylated Parkin expression, as demonstrated by Western blot assays (Fig. 4**C, D3–D5**). Changes in the Nrf2/Keap1 ratio, which is a main sensor system for the antioxidative response, were also observed. Notably, Nrf2 expression was reduced, and mitoQ administration largely reversed this change (Fig. 4**A, B2, C and D2**), results that paralleled those pertaining to PINK and Parkin expression. In contrast, Keap1, which is a negative regulator of Nrf2, was significantly up-regulated in the kidneys of db/db mice. This change was notably inhibited by mitoQ treatment (Fig. 4**A, B1, C and D1**). These results suggest that mitoQ regulates tubular mitophagy in diabetic kidneys via the Nrf2/Keap1 and PINK/Parkin pathways.

3.5. Effect of MitoQ on mitochondrial dysfunction, ROS production and apoptosis in HK-2 cells subjected to HG exposure

Immunoblotting demonstrated notable decreases in LC3II, PINK and Nrf2 expression levels in the nuclei of HK-2 cells, dose- and time-dependent changes induced by HG treatment (Fig. 5**A–B, A1–B1**). H2-DCFDA and MitoSOX demonstrated increases in intercellular and mitochondrial ROS levels in HK-2 cells exposed to HG conditions (Fig. 5**C, D1-D2**), and TUNEL assays demonstrated a significant increase in cell apoptosis induced by HG exposure (Fig. 5**C, D3**), an increase accompanied by up-regulated cleaved caspase-3 expression, which was detected using immunoblot assay (Fig. 5**E, E3**). However, these changes were significantly attenuated by mitoQ treatment (Fig. 5**C, D1–D3 and E3**). Increased Drp1 expression levels were noted in HK-2 cells subjected to HG exposure, while notably reduced Mfn2 expression levels were noted in HK-2 cells subjected to these conditions. These effects were partially abolished by mitoQ treatment (Fig. 5**E, E1–E2**). Decreased $\triangle\Psi$m and ATP activity were observed in HK-2 cells exposed to HG conditions, and mitoQ treatment reversed these effects (Fig. 5**F and G**).

3.6. Effect of MitoQ on mitophagy and mitophagy-related protein expression in HK-2 cells subjected to HG exposure

Moderately intense punctuate green fluorescence representing LC3 expression was observed in HK-2 cells under basal conditions. This expression was significantly reduced under HG ambience but was restored with mitoQ treatment. Decreases in LC3 expression and MitoRed staining were observed in merged photographs of HK-2 cells exposed to HG conditions, and mitoQ treatment dramatically reversed these decreases (Fig. 6**A**). Contrasting results were observed with p62 and MitoTracker double-staining (Fig. 6**A**). Western blot analysis demonstrated decreased LC3 expression and increased p62 expression in HK-2 cells subjected to HG exposure. These changes were partially abolished with mitoQ treatment (Fig. 6**C, D1 and D2**). Marked reductions in PINK expression intensity were observed via confocal microscopy in HK-2 cells exposed to HG. PINK expression was notably restored with mitoQ administration (Fig. 6**B**). Immunoblot assays confirmed the alterations in PINK, Parkin, p-Parkin and TOM20 expression in HK-2 cells exposed to HG conditions and the restoration of the expression of these proteins following mitoQ treatment (Fig. 6**C, D3-D5**). In addition, the abovementioned mitophagic defects were accompanied by significantly increased numbers of fragmented mitochondria in tubular cells incubated under HG conditions. These effects were dramatically reversed by mitoQ treatment (Fig. 6**E**).

3.7. MitoQ regulated PINK and Parkin expression via Nrf2/Keap1

Western blots demonstrated up-regulated Nrf2 and Keap1 expression in the cytoplasm of HK-2 cells incubated with HG. These changes were inhibited by mitoQ treatment. Nuclear Nrf2 expression was reduced but was restored by mitoQ treatment (Fig. 7**A, A1-A3**). Confocal microscopic images demonstrated decreased Nrf2 expression in the nuclear compartment of HK-2 cells subjected to HG exposure compared to HK-2 cells subjected to LG exposure. However, Nrf2 translocation increased concurrently with mitoQ-induced increases in nuclear Nrf2 expression (Fig. 7**B**). HG decreased Nrf2 activity in HK-2 cells. This activity was restored with mitoQ treatment (Fig. 7**C**). Notably, immunoprecipitation demonstrated an interaction between Nrf2 and Keap1 in HK-2 cells under basal conditions. This association was reduced in cells treated with mitoQ. Similar results regarding this reaction were also observed under HG conditions and mitoQ treatment (Fig. 7**D, D1 and D2**).

Western blotting demonstrated significant reductions in PINK and Parkin expression in HK-2 cells subjected to HG treatment, and mitoQ restored the expression of these proteins. This effect was augmented by transfection with Keap1 siRNA and attenuated by transfection with Nrf2 siRNA. However, the effects of Keap1 and Nrf2 on PINK and Parkin expression were dramatically neutralized by the simultaneous

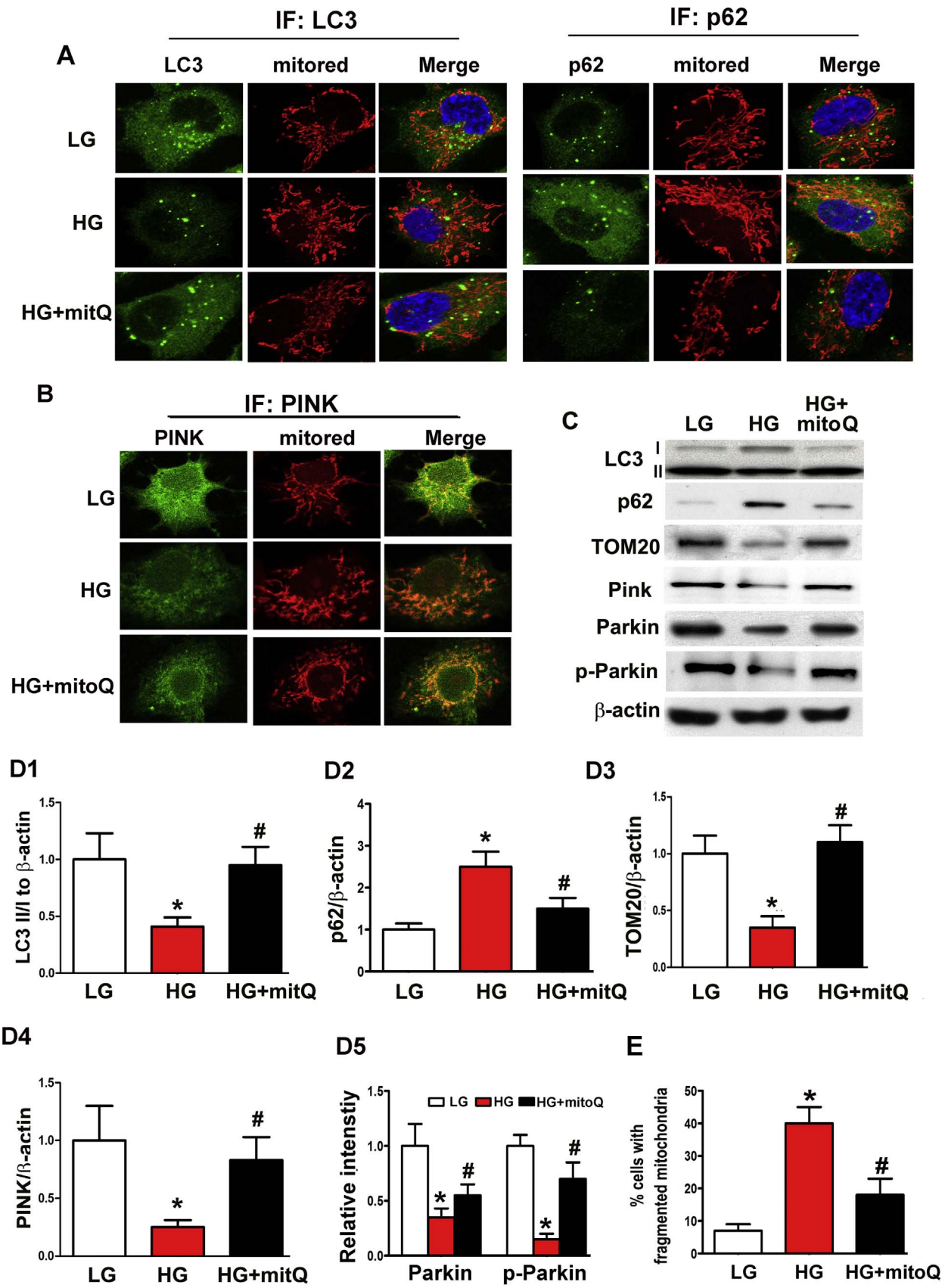

Fig. 6. The effect of mitoQ on defective mitophagy in HK-2 cells subjected to HG exposure. A: Cellular immunofluorescence showing that the colocalization intensity of LC3 and mitochondria (staining with MitoRed) was reduced in HK-2 cells incubated under HG conditions (left middle panels vs. top panels). This effect was partially reversed by mitoQ treatment (left bottom panels vs. middle panels). The opposite result was observed with respect to co-staining with a p62 antibody and MitoRed. B: Immunofluorescence staining with a PINK antibody and MitoRed revealing decreased colocalization intensity in HK-2 cells subjected to HG exposure (middle panels vs. top panels). Colocalization intensity was restored by mitoQ treatment (bottom panels vs. middle panels). C: Immunoblotting assay for LC3II, TOM20, PINK, Parkin and p-Parkin expression. D1-D5: Quantification of average Western blot band intensity. E. Percentage (%) of tubular cells with fragmented mitochondria. *P < 0.01 vs. LG; #P < 0.01 vs. HG, n=3.

co-transfection of Keap1 siRNA and Nrf2 siRNA (Fig. 7**E andE1**). Similarly, HG decreased PINK mRNA expression levels in HK-2 cells, and mitoQ treatment reversed these decreases. The increases in PINK mRNA levels facilitated by mitoQ were enhanced further by Keap1 siRNA transfection under HG exposure but were inhibited by Nrf2 siRNA. PINK transcription was also neutralized by Keap1 siRNA and

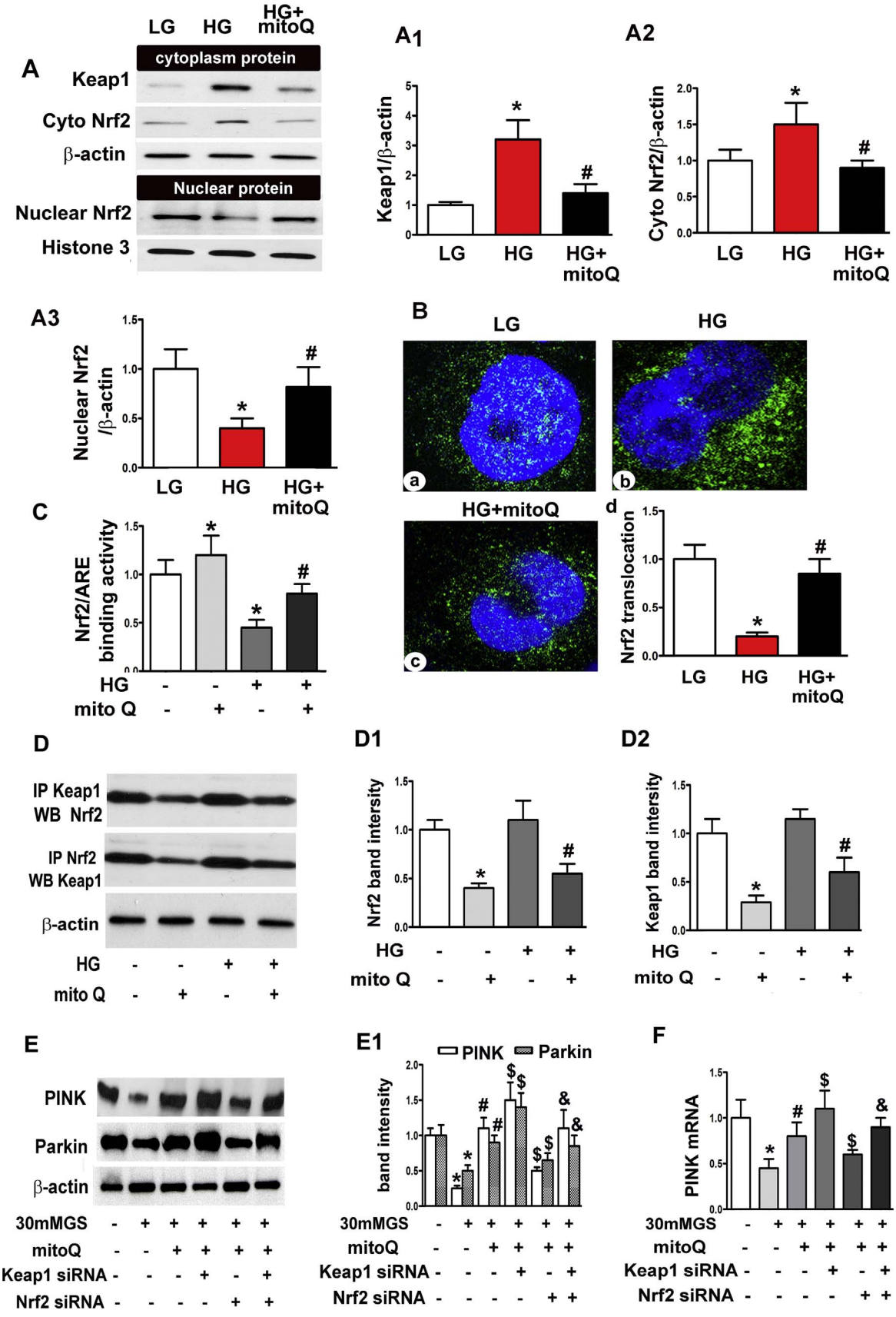

Fig. 7. The restorative effect of mitoQ on PINK and Parkin expression was mediated in part by Nrf2/Keap1. A: Immunoblotting assay for Keap1 and Nrf2 expression, which showed that mitoQ inhibited Keap1 and cytoplasmic Nrf2 expression in HK-2 cells exposed to HG and restored nuclear Nrf2 expression. A1-A3: Quantification of average Western blot band intensity. B: Immunofluorescence assay for Nrf2 showing decreased antibody staining intensity in HK-2 cells after incubation under HG conditions. MitoQ up-regulated the inhibition of Nrf2 intensity in HG-exposed cells. C: Bar graphs depicting Nrf2 binding to the ARE. D: The interaction between Keap1 and Nrf2 in HK-2 cells subjected to HG exposure with or without mitoQ was assessed using IP. D1 and D2: Quantification of the intensity of the interaction between Keap1 and Nrf2 using IP. E: Western blot analysis revealed that mitoQ restored PINK and Parkin expression in HK-2 cells exposed to HG, an effect that was partially abolished by transfection with Keap1 siRNA or Nrf2 siRNA. E1: Quantification of average Western blot band intensity. F: Similar results were observed for PINK mRNA expression, as demonstrated by real-time PCR. $^{*}P < 0.01$ vs. LG; $^{\#}P < 0.01$ vs. HG, $^{\$}P < 0.05$ compared to HG+mitoQ. $^{\&}P < 0.05$ compared to HG+mitoQ+Nrf2 siRNA. n=3.

Nrf2 siRNA co-transfection (Fig. 7**F**).

3.8. MitoQ restored mitophagy, oxidative stress and apoptosis in HK-2 cells subjected to HG exposure in part via Nrf2 and PINK

Nrf2 and PINK siRNAs were used to examine whether and how Nrf2 and PINK mediate the effects of mitoQ on tubular cells under HG conditions. Confocal imaging revealed that the merged intensity of LC3 and MitoTracker staining was significantly decreased in HK-2 cells under HG conditions but was restored by treatment with mitoQ. This effect was partially abolished by Nrf2 siRNA or PINK siRNA transfection (Fig. 8**A**). Conversely, mitoQ inhibited HG-induced intercellular ROS, mitochondrial ROS and apoptosis in HK-2 cells. These effects were attenuated by Nrf2 siRNA or PINK siRNA transfection (Fig. 8**A–D**). Western blot assays demonstrated that the HG-induced decreases in LC3II and TOM20 expression were reversed by mitoQ and were partially abolished by Nrf2 siRNA or PINK siRNA transfection. Contrasting results were observed for p62, Drp1 and caspase 3 expression in cells transfected with Nrf2 siRNA or PINK siRNA (Fig. 8**E, E1–E5**). These results suggest that MitoQ regulates mitophagy and attenuates tubular cell oxidative stress and apoptosis in part via the Nrf2/PINK pathway.

4. Discussion

The present study demonstrated that mitoQ administration dramatically reversed diabetic mouse kidney tubular damage via a reduction in oxidative stress in tubular cells. MitoQ regulated tubular cell mitophagy, a phenomenon that was accompanied by ameliorations of mitochondrial fragmentation and cell apoptosis. We also observed that Nrf2 contributed to this process by regulating the mitophagy-related protein PINK in *in vitro* and *in vivo* studies. These results are indicative of the existence of a novel mechanism by mitoQ protects against hyperglycemia-induced oxidative injury in tubular cells to maintain mitochondrial quality and also partially mediates mitophagy via Nrf2/PINK.

Diabetic tubulopathy has been increasingly implicated in DKD development. [35,36] Tubular injury contributes to primary renal injury, rather than secondary injury, in the pathogenesis of DKD, which is reflected by the fact that tubular damage markers appear before microalbuminuria. [37–40] The mechanisms underlying these phenomena are not fully clear, but others and our previous studies have demonstrated that dysfunctional mitochondria play a crucial role in this process. [6–9] Increasing evidence indicates that mitochondrial ROS overproduction, decreases in ATP activity and increases in mitochondrial fragmentation may be related to tubular cell damage and apoptosis in DKD. [6,7,9,41] However, whether inhibiting mitochondrial ROS production reverses tubular damage via mitochondrial quality control regulation is not known.

Conventional antioxidants may exhibit beneficial effects that decrease tubular oxidative damage, but these antioxidants are not effective clinically, largely because they are not effectively taken up by mitochondria *in vivo*. [21,42,43] In this study, we used the mitochondria-targeted antioxidant mitoQ to overcome this limitation. [21,31] Pre-treatment with mitoQ alleviated tubular damage in db/db mice, a change reflected by deceases in the levels of tubular injury markers, such as β-NAG. Notably, mitochondrial oxidative stress, mitochondrial fragmentation and mitochondrial dysfunction amelioration were accompanied by lower apoptosis levels in tubular cells under hyperglycemic conditions. Urine albumin excretion and kidney histological changes in db/db mice were attenuated by mitoQ treatment **(**Figs. 1, 2 and 5). These results are consistent with those of a previous report regarding type I diabetic mice. [22] Our results provide better complementary evidence of the effects of mitoQ with respect to protecting against tubular damage under hyperglycemic conditions using *in vitro* and different animal model studies.

Mitophagy is essential for the clearance of damaged mitochondria and is a critical component of mitochondrial quality control and oxidative stress. [44–47] There are limited data on the role of mitophagy in DKD progression and whether targeting mitophagy regulates renal pathological changes in DKD. Therefore, we investigated the protective effects of mitoQ on tubular cells and whether this effect was achieved by regulating mitophagy under hyperglycemia conditions. PINK1/Parkin is the most well understood mitophagy pathway. [12,45] PINK1 is activated on the surface of depolarized mitochondria and induces Parkin translocation and activation, which eventually leads to mitochondrial protein (e.g., TOM20 and Mfn2) degradation. The findings of a previous study suggested that D-glucarate restored tubular cell mitophagy by inhibiting MIOX in a Pink1-dependent manner under diabetic conditions. [3] We demonstrated for the first time that mitophagy was decreased in db/db mice, a type II diabetic mouse model, and in mice subjected to HG exposure (Figs. 3 and 4). These results are consistent with those of previous reports involving type I diabetic mice [3,13] and are also consistent with previous observations regarding diabetic hearts and skeletal muscles. [48,49] MitoQ dramatically reversed mitophagy by up-regulating PINK and Parkin expression (Figs. 5 and 6), findings indicating that mitoQ plays another role in tubular injury besides inhibiting mitochondrial ROS production in DKD.

We also investigated the molecular mechanisms by which mitoQ modulates tubular cell mitophagy under hyperglycemic conditions. Nrf2 is an antioxidant and a crucial factor in oxidative stress and metabolism. [50,51] Moreover, Nrf2 is associated with Keap1 under physiological conditions and is released to activate target gene transcription during oxidative stress. [51] Genetic activation of Nrf2 markedly suppressed the onset of diabetes, [50] and depletion of Nrf2 increased renal oxidative stress in STZ-induced diabetic mice. [43] Decreased Nrf2 expression and translocation were associated with tubular injury in STZ-induced diabetic rats and under HG conditions. These changes were modulated by the Sirt1/NF-κB/miR-29/Keap1 pathway. [52] However, the role of Nrf2 in the effects of mitoQ on tubular mitophagy and oxidative stress in DKD is not clear.

Nrf2 expression and activity were up-regulated with mitoQ treatment, changes accompanied by a significant restoration in autophagy levels in breast cells.[23]Moreover, Nrf2 positively regulated PINK1 transcription and attenuated oxidative stress-associated cell death. [53] We observed a tighter interaction between Nrf2 and Keap1 under HG conditions. This interaction was accompanied by decreased Nrf2 expression and translocation in tubular cells. However, these effects were dramatically reversed by mitoQ treatment. MitoQ also restored HG-induced PINK mRNA and protein expression, an effect that was partially abolished by Nrf2 siRNA (Fig. 7). The effects of mitoQ on mitophagy and mitochondrial function were neutralized by Nrf2 or PINK siRNA under HG conditions (Fig. 8). These data indicate that

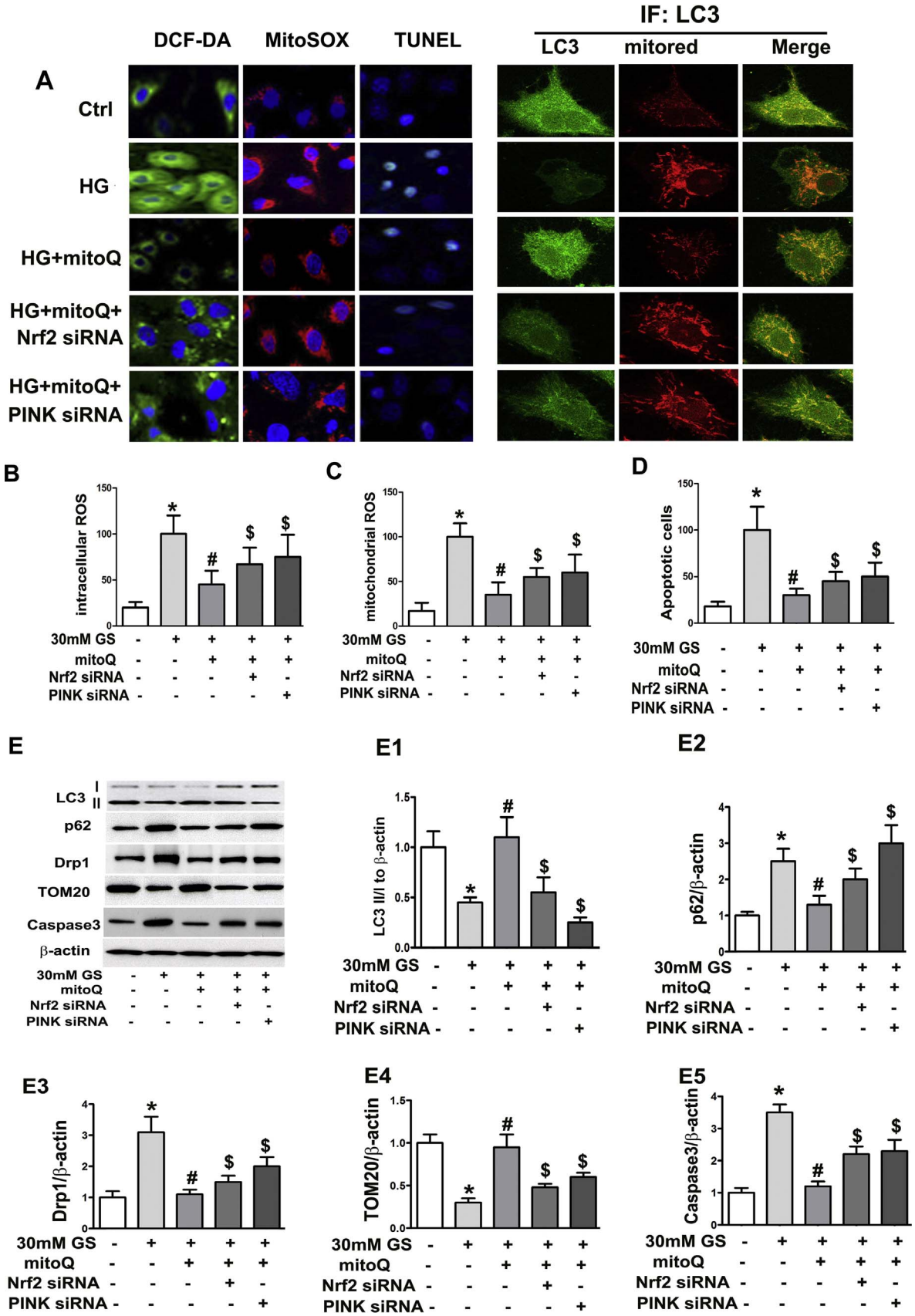

Fig. 8. Restorative effect of mitoQ on mitophagy, ROS production and apoptosis via Nrf2 and PINK. A: Confocal microscopic image showing that mitoQ ameliorated intracellular ROS production, mitochondrial ROS production and apoptosis in HK-2 cells subjected to HG exposure, as demonstrated by H2-DCFDA, MitoSOX and TUNEL assays, respectively. These effects were partially blocked by Nrf2 siRNA or PINK-siRNA. Transfection with Nrf2 siRNA or PINK-siRNA also attenuated LC3 and mitochondria colocalization intensity in cells treated with mitoQ under HG conditions. B–D: Bar graphs represent intracellular and mitochondrial ROS and apoptosis levels, as demonstrated using H2-DCFDA, MitoSOX and TUNEL assays. E: The effect of Nrf2 siRNA or PINK-siRNA on LC3II, p62, Drp1, and TOM20 expression in HK-2 cells subjected to HG exposure with or without mitoQ using immunoblot assays. E1-E5: Quantification of average Western blot band intensities. *P < 0.05 compared to LG; $^{\#}$ P < 0.05 compared to HG. $^{\$}$P < 0.05 compared to HG+mitoQ.

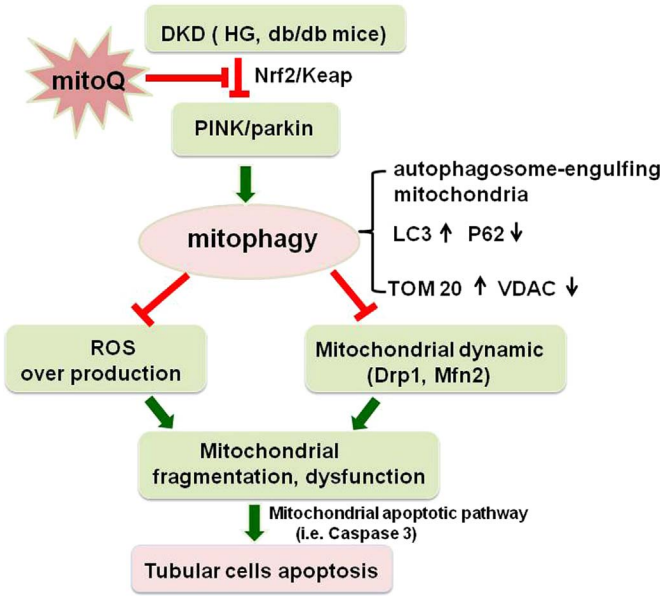

Fig. 9. Schematic diagram depicting the possible molecular mechanisms by which mitoQ prevents renal tubular cell injury by maintaining mitochondrial integrity under HG conditions. Under HG conditions, nuclear Nrf2 expression and activity are down-regulated in tubular cells, which decreases PINK1 transcription and subsequent Parkin phosphorylations and then leads to defective mitophagy. This insufficient mitophagy results in ROS overproduction and aberrant mitochondrial dynamics characterized by Drp1 activation and Mfn2 suppression, changes accompanied by mitochondrial dysfunction, fragmented mitochondria accumulation and mitochondrial apoptotic pathway activation, i.e., caspase 3 release, which eventually leads to cell apoptosis. Interestingly, mitoQ treatment increases the dissociation of Nrf2 from Keap1, and the nuclear location of the former up-regulates the transcription of PINK and restores mitophagy, which maintains mitochondrial quality control, thereby attenuating hyperglycemia-induced tubular injury and apoptosis.

Nrf2 contributed to the restoration of mitophagy and mitochondrial quality by regulating PINK transcription in tubular cells treated with mitoQ in DKD. Despite our extensive investigatory efforts, certain issues remain unclear. For instance, the mechanism by which mitoQ modulates Nrf2 and Keap remains to be delineated. Additionally, whether mitoQ plays a potential protective role in tubular injury in diabetic patients is worthy of further study.

In conclusion, this study demonstrated the novel beneficial effects of mitoQ on tubular damage in DKD using *in vitro and in vivo* models. The mechanism underlying its effects may involve regulating mitochondrial quality control, a process that entails restoring mitophagy in tubular cells via Nrf2-mediated regulation of PINK transcription and ameliorating mitochondrial oxidative stress and aberrant mitochondrial dynamics, which eventually results in tubular injury and apoptosis attenuation under HG conditions (Fig. 9). These results suggest that the mitochondrial-targeted antioxidant mitoQ is an attractive agent for preventing tubular injury in DKD.

Funding

This work was supported by the Fund of the National Foundation Committee of Natural Sciences of China (81370832, 81470960, 81570658)) and ZR2013HM093.

Conflicts of Interest

No potential conflicts of interest relevant to this article are reported.

Author Contributions

L.X., X.X, F.Z., M.W., Y.X., D.T., J.W., and Y.Q. generated the data for the manuscript. C.T., L.H., Z.Z., F.L., and Y.L. discussed the results of the manuscript. A.G, Z.D., and L.S. partially edited the manuscript. L.X. is the guarantor of this work and, as such, had full access to all the data for the study and takes responsibility for its integrity and for the accuracy of the data analysis.

References

[1] K. Simpson, A. Wonnacott, D.J. Fraser, T. Bowen, MicroRNAs in Diabetic Nephropathy: From Biomarkers to Therapy, Current diabetes reports 16 (2016) 35.
[2] J. Watanabe, Y. Takiyama, J. Honjyo, Y. Makino, Y. Fujita, M. Tateno, M. Haneda, Role of IGFBP7 in Diabetic Nephropathy: TGF-beta1 Induces IGFBP7 via Smad2/4 in Human Renal Proximal Tubular Epithelial Cells, PloS one 11 (2016) e0150897.
[3] M. Zhan, I.M. Usman, L. Sun, Y.S. Kanwar, Disruption of renal tubular mitochondrial quality control by Myo-inositol oxygenase in diabetic kidney disease, Journal of the American Society of Nephrology: JASN 26 (2015) 1304–1321.
[4] G.C. Higgins, M.T. Coughlan, Mitochondrial dysfunction and mitophagy: the beginning and end to diabetic nephropathy?, British journal of pharmacology 171 (2014) 1917–1942.
[5] L. Sun, R.K. Dutta, P. Xie, Y.S. Kanwar, myo-Inositol Oxygenase Overexpression Accentuates Generation of Reactive Oxygen Species and Exacerbates Cellular Injury following High Glucose Ambience: A new mechanism relevant to the pathogenesis of diabetic nephropathy, The Journal of biological chemistry 291 (2016) 5688–5707.
[6] M.T. Coughlan, T.V. Nguyen, S.A. Penfold, G.C. Higgins, V. Thallas-Bonke, S.M. Tan, N.J. Van Bergen, K.C. Sourris, B.E. Harcourt, D.R. Thorburn, I.A. Trounce, M.E. Cooper, J.M. Forbes, Mapping time-course mitochondrial adaptations in the kidney in experimental diabetes, Clinical science 130 (2016) 711–720.
[7] L. Sun, L. Xiao, J. Nie, F.Y. Liu, G.H. Ling, X.J. Zhu, W.B. Tang, W.C. Chen, Y.C. Xia, M. Zhan, M.M. Ma, Y.M. Peng, H. Liu, Y.H. Liu, Y.S. Kanwar, p66Shc mediates high-glucose and angiotensin II-induced oxidative stress renal tubular injury via mitochondrial-dependent apoptotic pathway, American journal of physiology Renal physiology 299 (2010) F1014–F1025.
[8] Y. Hou, S. Li, M. Wu, J. Wei, Y. Ren, C. Du, H. Wu, C. Han, H. Duan, Y. Shi, Mitochondria-targeted peptide SS-31 attenuates renal injury via an antioxidant effect in diabetic nephropathy, American journal of physiology Renal physiology 310 (2016) F547–F559.
[9] L. Xiao, X. Zhu, S. Yang, F. Liu, Z. Zhou, M. Zhan, P. Xie, D. Zhang, J. Li, P. Song, Y.S. Kanwar, L. Sun, Rap1 ameliorates renal tubular injury in diabetic nephropathy, Diabetes 63 (2014) 1366–1380.
[10] J. Zhu, K.Z. Wang, C.T. Chu, After the banquet: mitochondrial biogenesis, mitophagy, and cell survival, Autophagy 9 (2013) 1663–1676.
[11] M. Ishihara, M. Urushido, K. Hamada, T. Matsumoto, Y. Shimamura, K. Ogata, K. Inoue, Y. Taniguchi, T. Horino, M. Fujieda, S. Fujimoto, Y. Terada, Sestrin-2 and BNIP3 regulate autophagy and mitophagy in renal tubular cells in acute kidney injury, American journal of physiology Renal physiology 305 (2013) F495–F509.
[12] J. Gatliff, M. Campanella, TSPO is a REDOX regulator of cell mitophagy, Biochemical Society transactions 43 (2015) 543–552.
[13] C. Huang, Y. Zhang, D.J. Kelly, C.Y. Tan, A. Gill, D. Cheng, F. Braet, J.S. Park, C.M. Sue, C.A. Pollock, X.M. Chen, Thioredoxin interacting protein (TXNIP) regulates tubular autophagy and mitophagy in diabetic nephropathy through the mTOR signaling pathway, Scientific reports 6 (2016) 29196.
[14] W.Y. Wani, S. Gudup, A. Sunkaria, A. Bal, P.P. Singh, R.J. Kandimalla, D.R. Sharma, K.D. Gill, Protective efficacy of mitochondrial targeted antioxidant MitoQ against dichlorvos induced oxidative stress and cell death in rat brain, Neuropharmacology 61 (2011) 1193–1201.
[15] A.O. Oyewole, M.A. Birch-Machin, Mitochondria-targeted antioxidants, FASEB J 29 (2015) 4766–4771.
[16] H. Rehman, Q. Liu, Y. Krishnasamy, Z. Shi, V.K. Ramshesh, K. Haque, R.G. Schnellmann, M.P. Murphy, J.J. Lemasters, D.C. Rockey, Z. Zhong, The mitochondria-targeted antioxidant MitoQ attenuates liver fibrosis in mice, Int J Physiol Pathophysiol Pharmacol 8 (2016) 14–27.
[17] X. Yin, M. Manczak, P.H. Reddy, Mitochondria-targeted molecules MitoQ and SS31 reduce mutant huntingtin-induced mitochondrial toxicity and synaptic damage in Huntington's disease, Hum Mol Genet. 25 (2016) 1739–1753.
[18] D. Graham, N.N. Huynh, C.A. Hamilton, E. Beattie, R.A. Smith, H.M. Cocheme, M.P. Murphy, A.F. Dominiczak, Mitochondria-targeted antioxidant MitoQ10 improves endothelial function and attenuates cardiac hypertrophy, Hypertension 54 (2009) 322–328.
[19] E.J. Gane, F. Weilert, D.W. Orr, G.F. Keogh, M. Gibson, M.M. Lockhart, C.M. Frampton, K.M. Taylor, R.A. Smith, M.P. Murphy, The mitochondria-targeted anti-oxidant mitoquinone decreases liver damage in a phase II study of hepatitis C patients, Liver Int 30 (2010) 1019–1026.
[20] T. Mitchell, D. Rotaru, H. Saba, R.A. Smith, M.P. Murphy, L.A. MacMillan-Crow, The mitochondria-targeted antioxidant mitoquinone protects against cold storage injury of renal tubular cells and rat kidneys, J Pharmacol Exp Ther 336 (2011) 682–692.
[21] A.J. Dare, E.A. Bolton, G.J. Pettigrew, J.A. Bradley, K. Saeb-Parsy, M.P. Murphy, Protection against renal ischemia-reperfusion injury in vivo by the mitochondria targeted antioxidant MitoQ, Redox Biol. 5 (2015), 2015 163-8.
[22] B.K. Chacko, C. Reily, A. Srivastava, M.S. Johnson, Y. Ye, E. Ulasova, A. Agarwal, K.R. Zinn, M.P. Murphy, B. Kalyanaraman, V. Darley-Usmar, Prevention of

diabetic nephropathy in Ins2(+/)(-)(AkitaJ) mice by the mitochondria-targeted therapy MitoQ, Biochem. J 432 (2010) 9–19.
[23] Y. Gonzalez, B. Aryal, L. Chehab, V.A. Rao, Atg7- and Keap1-dependent autophagy protects breast cancer cell lines against mitoquinone-induced oxidative stress, Oncotarget 5 (2014) 1526–1537.
[24] L. Sun, D. Zhang, F. Liu, X. Xiang, G. Ling, L. Xiao, Y. Liu, X. Zhu, M. Zhan, Y. Yang, V.K. Kondeti, Y.S. Kanwar, Low-dose paclitaxel ameliorates fibrosis in the remnant kidney model by down-regulating miR-192, The Journal of pathology 225 (2011) 364–377.
[25] X. Wang, E. Shen, Y. Wang, Z. Jiang, D. Gui, D. Cheng, T. Chen, N. Wang, MiR-196a Regulates High Glucose-Induced Mesangial Cell Hypertrophy by Targeting p27kip1, Journal of laboratory automation 20 (2015) 491–499.
[26] M. Jiang, K. Liu, J. Luo, Z. Dong, Autophagy is a renoprotective mechanism during in vitro hypoxia and in vivo ischemia-reperfusion injury, The American journal of pathology 176 (2010) 1181–1192.
[27] R.K. Emaus, R. Grunwald, J.J. Lemasters, Rhodamine 123 as a probe of transmembrane potential in isolated rat-liver mitochondria: spectral and metabolic properties, Biochimica et biophysica acta 850 (1986) 436–448.
[28] J. Li, W. He, B. Liao, J. Yang, FFA-ROS-P53-mediated mitochondrial apoptosis contributes to reduction of osteoblastogenesis and bone mass in type 2 diabetes mellitus, Scientific reports 5 (2015) 12724.
[29] J. Gatliff, D. East, J. Crosby, R. Abeti, R. Harvey, W. Craigen, P. Parker, M. Campanella, TSPO interacts with VDAC1 and triggers a ROS-mediated inhibition of mitochondrial quality control, Autophagy 10 (2014) 2279–2296.
[30] C. Snyder, K. Mantione, The effects of morphine on Parkinson's-related genes PINK1 and PARK2, Medical science monitor basic research 20 (2014) 63–69.
[31] I.M. Aparicio, J. Espino, I. Bejarano, A. Gallardo-Soler, M.L. Campo, G.M. Salido, J.A. Pariente, F.J. Pena, J.A. Tapia, Autophagy-related proteins are functionally active in human spermatozoa and may be involved in the regulation of cell survival and motility, Scientific reports 6 (2016) 33647.
[32] Q.Q. Li, L. Zhang, H.Y. Wan, M. Liu, X. Li, H. Tang, CREB1-driven expression of miR-320a promotes mitophagy by down-regulating VDAC1 expression during serum starvation in cervical cancer cells, Oncotarget 6 (2015) 34924–34940.
[33] L. Xu, Q. Fan, X. Wang, X. Zhao, L. Wang, Inhibition of autophagy increased AGE/ROS-mediated apoptosis in mesangial cells, Cell death & disease 7 (2016) e2445.
[34] C.B. McLeland, J. Rodriguez, S.T. Stern, Autophagy monitoring assay: qualitative analysis of MAP LC3-I to II conversion by immunoblot, Methods in molecular biology 697 (2011) 199–206.
[35] T. Fiseha, Z. Tamir, Urinary Markers of TubularInjury in Early Diabetic Nephropathy, International journal of nephrology 2016 (2016) 4647685.
[36] J. Slyne, C. Slattery, T. McMorrow, M.P. Ryan, New developments concerning the proximal tubule in diabetic nephropathy: in vitro models and mechanisms, Nephrology, dialysis, transplantation: official publication of the European Dialysis and Transplant Association - European Renal Association 30 (Suppl 4) (2015) iv60-7.
[37] J.V. Bonventre, Can we target tubular damage to prevent renal function decline in diabetes?, Seminars in nephrology 32 (2012) 452–462.
[38] S.C. Tang, J.C. Leung, K.N. Lai, Diabetic tubulopathy: an emerging entity, Contributions to nephrology 170 (2011) 124–134.
[39] S.C. Tang, K.N. Lai, The pathogenic role of the renal proximal tubular cell in diabetic nephropathy, Nephrology, dialysis, transplantation: official publication of the European Dialysis and Transplant Association - European Renal Association 27 (2012) 3049–3056.
[40] J.A. de Carvalho, E. Tatsch, B.S. Hausen, Y.S. Bollick, M.B. Moretto, T. Duarte, M.M. Duarte, S.W. Londero, M.O. Premaor, F.V. Comim, J.R. Delanghe, R.N. Moresco, Urinary kidney injury molecule-1 and neutrophil gelatinase-associated lipocalin as indicators of tubular damage in normoalbuminuric patients with type 2 diabetes, Clinical biochemistry 49 (2016) 232–236.
[41] M.D. Covington, R.G. Schnellmann, Chronic high glucose downregulates mitochondrial calpain 10 and contributes to renal cell death and diabetes-induced renal injury, Kidney international 81 (2012) 391–400.
[42] H.M. Cocheme, M.P. Murphy, Can antioxidants be effective therapeutics?, Current opinion in investigational drugs 11 (2010) 426–431.
[43] K. Yoh, A. Hirayama, K. Ishizaki, A. Yamada, M. Takeuchi, S. Yamagishi, N. Morito, T. Nakano, M. Ojima, H. Shimohata, K. Itoh, S. Takahashi, M. Yamamoto, Hyperglycemia induces oxidative and nitrosative stress and increases renal functional impairment in Nrf2-deficient mice, Genes to cells: devoted to molecular & cellular mechanisms 13 (2008) 1159–1170.
[44] A. Diot, K. Morten, J. Poulton, Mitophagy plays a central role in mitochondrial ageing, Mammalian genome: official journal of the International Mammalian Genome Society 27 (2016) 381–395.
[45] Q. Liang, S. Kobayashi, Mitochondrial quality control in the diabetic heart, Journal of molecular and cellular cardiology 95 (2016) 57–69.
[46] S. Aggarwal, P. Mannam, J. Zhang, Differential Regulation of Autophagy and Mitophagy in Pulmonary Diseases, American journal of physiology Lung cellular and molecular physiology 2016:ajplung 00128 (2016).
[47] A. Hjelmeland, J. Zhang, Metabolic, autophagic, and mitophagic activities in cancer initiation and progression, Biomedical journal 39 (2016) 98–106.
[48] Y. Tang, J. Liu, J. Long, Phosphatase and tensin homolog-induced putative kinase 1 and Parkin in diabetic heart: Role of mitophagy, Journal of diabetes investigation 6 (2015) 250–255.
[49] C. Scheele, A.R. Nielsen, T.B. Walden, D.A. Sewell, C.P. Fischer, R.J. Brogan, N. Petrovic, O. Larsson, P.A. Tesch, K. Wennmalm, D.S. Hutchinson, B. Cannon, C. Wahlestedt, B.K. Pedersen, J.A. Timmons, Altered regulation of the PINK1 locus: a link between type 2 diabetes and neurodegeneration?, FASEB J 21 (2007) 3653–3665.
[50] A. Uruno, Y. Furusawa, Y. Yagishita, T. Fukutomi, H. Muramatsu, T. Negishi, A. Sugawara, T.W. Kensler, M. Yamamoto, The Keap1-Nrf2 system prevents onset of diabetes mellitus, Molecular and cellular biology 33 (2013) 2996–3010.
[51] H. Yang, Y. Mao, B. Tan, S. Luo, Y. Zhu, The protective effects of endogenous hydrogen sulfide modulator, S-propargyl-cysteine, on high glucose-induced apoptosis in cardiomyocytes: A novel mechanism mediated by the activation of Nrf2, European journal of pharmacology 761 (2015) 135–143.
[52] L. Zhou, D.Y. Xu, W.G. Sha, L. Shen, G.Y. Lu, X. Yin, M.J. Wang, High glucose induces renal tubular epithelial injury via Sirt1/NF-kappaB/microR-29/Keap1 signal pathway, Journal of translational medicine 13 (2015) 352.
[53] H. Murata, H. Takamatsu, S. Liu, K. Kataoka, N.H. Huh, M. Sakaguchi, NRF2 Regulates PINK1 expression under oxidative stress conditions, PloS one 10 (2015) e0142438.